J MATER SCI 41 (2006) 709–717

Silicon-substituted hydroxyapatite (SiHA): A novel calcium phosphate coating for biomedical applications

E. S. THIAN*, J. HUANG, M. E. VICKERS, S. M. BEST, Z. H. BARBER, W. BONFIELD
Department of Materials Science and Metallurgy, University of Cambridge, Pembroke Street, Cambridge, CB2 3QZ, UK
E-mail: est23@cam.ac.uk

Hydroxyapatite [$Ca_{10}(PO_4)_6(OH)_2$], (HA) is similar in composition to bone mineral and has been found to promote new bone formation when implanted in a skeletal defect. However, its use in biomedical applications is limited by its relatively slow rate of biological interaction, and there is also a requirement to improve the success rate of HA implants in younger active patients, particularly where implants will be in place long-term. The addition of silicon (Si) into HA has been demonstrated to enhance the speed, and quality of the bone repair process. This paper describes the synthesis and detailed characterisation of nanocrystalline silicon-substituted hydroxyapatite (SiHA) thin coatings applied to a titanium substrate via a magnetron co-sputtering process. Amorphous SiHA coatings ($\sim$1 μm thick) with varying Si content up to 4.9 wt% were produced before being transformed into crystalline films by heat-treatment. The crystalline coating was characterised by X-ray diffraction (XRD) and infrared (IR) analysis, and confirmed to be a single-phase apatite. The substitution of Si into HA resulted in an increase in both the *a*- and *c*-axes of the unit cell parameters, but a decrease in the crystallite size, with increasing Si substitution. This substitution also caused a decrease in the intensities of both the O–H and P–O bands in the IR spectra. Hence, these findings confirmed that the crystal structure of HA was altered with Si substitution. *In vitro* cell culture work showed that these SiHA thin coatings exhibited enhanced bioactivity and biofunctionality. An increase in the attachment and growth of human osteoblast-like (HOB) cells on these coatings was observed throughout the culture period, with the formation of extracellular matrix. In addition, confocal microscopy revealed that HOBs developed mature cytoskeletons with clear evidence of actin stress fibres, along with defined cell nuclei.

1. Introduction

The demand for artificial medical implants has increased dramatically during the past three decades, owing to sport-related injuries and age-related diseases. Synthetic materials in the form of metals, ceramics or polymers have been used to restore and replace diseased or damaged tissues. Such materials must be non-toxic and biocompatible *in vivo*, such that no adverse host response is induced. Metals such as titanium (Ti) and its alloys have been commonly used for skeletal implants (in major load bearing prostheses) where relatively high mechanical strength is required. However, the surfaces of such materials are not generally osteoconductive (that is bone cells do not adhere, proliferate and differentiate to form extracellular matrix) and therefore exhibit relatively poor integration with the bone tissue at the implantation site [1]. To improve this bone-bonding ability (osteointegration) at the bone/implant interface, one approach is to apply a bioactive coating on the metal surface to encourage bone apposition rather than fibrous encapsulation. The calcium phosphate (CaP) family, and in particular hydroxyapatite (HA), has been chosen as a coating material because it is bioactive and osteoconductive, with a crystallographic and chemical composition approximating to that bone mineral [2]. HA

*Author to whom all correspondence should be addressed.
0022-2461
DOI: 10.1007/s10853-006-6489-8

has the chemical formula $Ca_{10}(PO_4)_6(OH)_2$, a Ca:P ratio of 10:6 (1.67), and a hexagonal crystallographic lattice with a space group $P6_3/m$ [3]. Recently, a study on HA-coated femoral stems for orthopaedic prostheses implanted in patients younger than fifty years, with a mean follow-up time of ten years showed excellent clinical survival rate of nearly 100% [4]. HA coatings have also been reported to improve fixation in orthopaedic implants, especially during the early stage of healing [5, 6].

In recent years, developments in novel bioactive coatings have led to an overall improvement in the performance of skeletal implants. Lacefield and Hench [7] have developed Bioglass® coatings on cobalt-chromium alloy substrates and demonstrated good glass-metal bond strength at the interface. Bioactive glass coatings have been shown to stimulate osteoblast (bone-forming cells) proliferation and differentiation *in vitro* [8, 9]. An *in vivo* study using a rabbit model showed direct formation of new bone tissue on coating, without the formation of fibrous connective tissue [10]. However, the presence of high levels of released silicon ions from the coating could contribute to apoptosis (cell death) [11–13].

An alternative way to accelerate skeletal fixation is via the incorporation of biological entities such as bone morphogenetic proteins (BMPs; which are capable of inducing rapid bone formation) or transforming growth factors (TGFs; which are capable of stimulating cell proliferation and differentiation) into the CaP coatings. Vehof *et al*. [14] demonstrated that the combination of CaP coating with BMPs had a beneficial effect on bone-inducing properties. HA-coated implants loaded with TGFs have been shown to stimulate bone formation in dogs *in vivo* [15]. However, the beneficial effects of these bioactive agents have been reported to decline during storage and sterilisation processes [16].

Recently, there has been increasing research interest concerning the effects of various ion substitutions, such as magnesium, silicon, fluorine and carbonate, on the bioactivity of HA; since these ions play a significant role in the biochemistry of bone tissues [17–20]. Studies by Carlisle [21–24] have shown the importance of silicon (Si) in bone formation and mineralisation. Carlisle demonstrated that Si is essential for growth, feathering and skeletal development in chicks. Chicks fed on an unsupplemented Si diet showed reduced growth, diminished feather development and significantly retarded skeletal development. In addition, an *in vitro* study has demonstrated that Si in the form of orthosilicic acid present in physiological concentrations of 5–20 μM enhanced osteoblastic differentiation and stimulated type I collagen synthesis in human osteoblast-like cells [25]. Recently, a number of studies introducing silicon-substituted hydroxyapatite (SiHA) have been reported and the material has been shown to enhance the rate and quality of bone tissue repair [26–28]. Thus, there is a logic in the development of novel substituted apatite coatings since they are likely to offer the potential of enhanced bioactivity. Until recently, little work has been directed towards the use of thin coatings of SiHA for potential applications in orthopaedic and dental implants [29, 30].

Plasma spraying is the most common technique to apply thick (50–200 μm) CaP coatings, owing to its suitability for large-scale production and economic efficiency [31, 32]. It is a technique in which a material powder, suspended in a carrier gas, is fed into the plasma and impinged in a molten state towards a surface, at high temperature and velocity. Although plasma-sprayed coatings have shown great benefits in encouraging bone growth around skeletal implants, this technique presents some drawbacks influencing the long-term performance and life-time of the implants [33, 34]. Poor coating-substrate adhesion, lack of coating uniformity in terms of morphology and crystallinity, and limitations on coating complex shapes have been associated with plasma-sprayed coatings [35–38]. Therefore, alternative coating techniques to apply SiHA are necessary. An innovative way is to use a magnetron co-sputtering technique to grow SiHA coatings at room temperature. It is a plasma vacuum coating technique whereby positively-charged ions are accelerated towards a target's surface. The impact of these ions will then produce sputtering of the surface, that is, 'knocking out' of individual atoms from the target. This technique has the advantages of achieving dense, uniform and well-adhered thin coatings, with the possibility of the addition of controlled levels of Si. The ability to produce thin, well-adhered coatings reduces the risk of delamination with the associated formation of HA debris during implant insertion, thereby decreasing polyethylene wear and hence osteolysis [39, 40]. This paper reports the properties of thin coatings made of SiHA by magnetron co-sputtering.

2. Materials and methods

2.1. Magnetron co-sputtering process

Commercially pure titanium (Ti, obtained from Advent Research Materials Ltd., UK) measuring 10 mm by 5 mm by 0.5 mm, were used as substrates. They were ground using silicon carbide paper of grade 1200. After grinding, the substrates were cleaned with acetone for 30 min in an ultrasonic bath, before rinsing with deionised water and dried. Pure silicon (Si, obtained from Goodfellow Cambridge Ltd., UK) and slip-cast phase-pure sintered hydroxyapatite (HA, obtained from Almath Crucibles Ltd., UK) measuring 55 mm by 35 mm by 2 mm, were used as the sputtering targets.

Magnetron co-sputtering was performed using a custom-built sputter deposition unit at room temperature (Fig. 1). The Ti substrates were placed on a substrate holder facing the targets, while the Si and HA

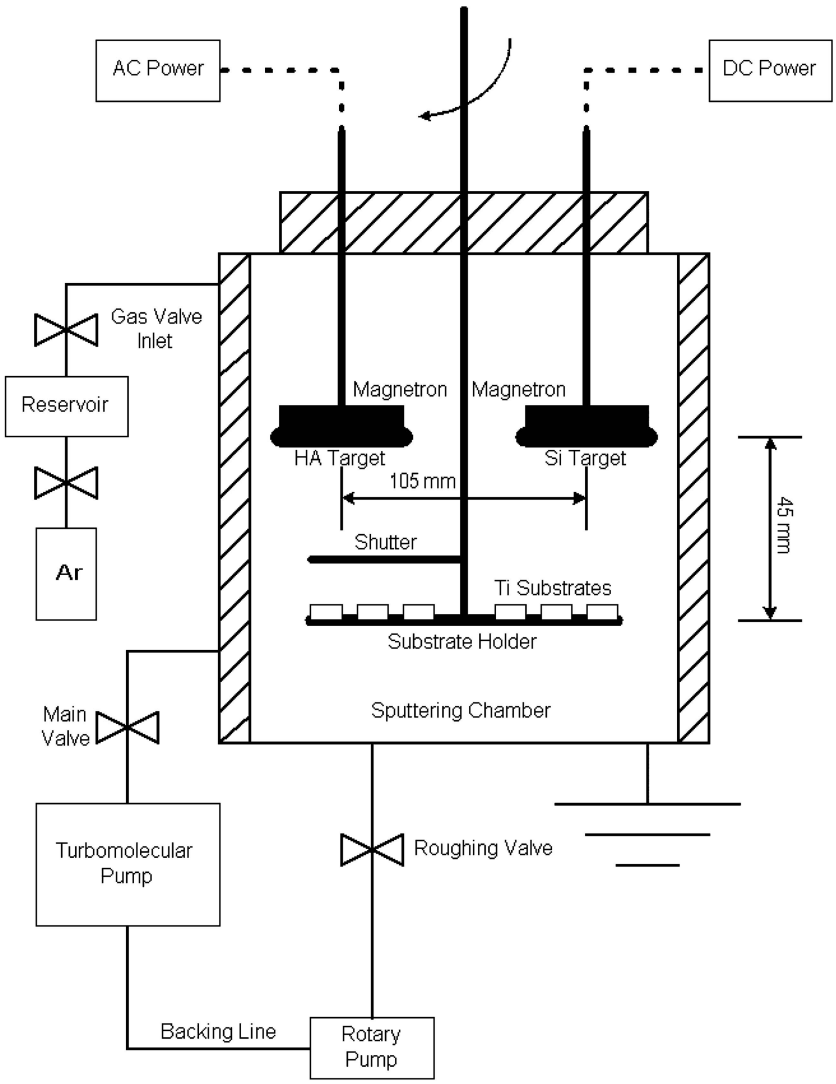

Figure 1 Schematic diagram of the magnetron co-sputtering system.

targets were held onto the two water-cooled magnetrons by means of spring clips. The target-target and target-substrate distances were kept constant at 105 mm and 45 mm, respectively for all runs. For each deposition run, a constant flow of high purity argon (Ar) gas was supplied into the chamber, bringing the working pressure to 0.6 Pa; and a sputtering time of 4 h was used. The coating composition was controlled by the relative discharge power supplied to each target. Three different direct current (dc) powers (3 W, 9 W and 15 W) were supplied to the Si target, whilst a radio frequency (rf: 13.56 MHz) power of 60 W was supplied to the HA target. The as-deposited coatings were then heat-treated in a water vapour-Ar atmosphere at 600°C for 3 h in a tube furnace.

2.2. Physicochemical analysis of SiHA

The coating thickness was determined by masking a portion of a Si substrate with a layer of aluminium foil during the deposition run and then removing the foil from the substrate, creating a step in the coating. This step was measured using a Talysurf 6 Stylus Surface Profilometer. A JEOL 6340F Field Emission Gun Scanning Electron Microscope (FE-SEM) equipped with an Energy Dispersive X-ray Spectrometer (EDS) was used to observe the coating morphology and to determine the weight percentage of Si in the coatings, at an accelerating voltage of 10 kV.

Changes in the structural composition of the coatings were identified using a Philips PW3020 Vertical X-ray Diffractometer (XRD) with CuK_α ($\lambda = 0.15405$ nm) radiation operating at 40 kV and 40 mA. Data were collected over a 2θ range of 20° to 40°, with a step size of 0.03° and a dwell time of 20 s. Phases were identified by comparison of the experimental data with the reference data from International Centre for Diffraction Data (ICDD) Standards. Peak widths were obtained by profile fitting and crystallite size (L_{001}) of the coatings was obtained using

Scherrer equation (without any correction for instrumental broadening):

$$L_{001} = \lambda/\beta \cos \theta \quad (1)$$

where λ is the X-ray wavelength (0.15405 nm) and β is the full width at half maximum of the diffraction line of 2θ (in radian). Calculations were performed for the (001) plane of HA ($2\theta = 25.879^\circ$). Determination of the unit cell parameters (a and c) of the coatings was made by Rietveld refinement of the X-ray diffraction data collected over a 2θ range of 20° to 80°, with a step size of 0.03° and a dwell time of 20 s. Refinement software X'Pert Plus [41] was used based on the structural data for HA of Kay *et al.* [42]. The following parameters were refined: background parameters, scale factors, zero points, lattice parameters and orientation parameters.

A Bio-Rad FTS6000 Fourier Transform Infrared Spectrometer (FTIR), utilising a grazing angle technique, was used to analyse the molecular structure of the coatings. The spectra were collected over a range of 700 cm^{-1} to 4000 cm^{-1} to monitor any changes in the phosphate or hydroxyl groups. A resolution of 4 cm^{-1} was used and the samples were scanned 64 times to increase the signal-to-noise ratio. An uncoated Ti substrate was used as a background subtraction.

2.3. Cell culture work

Primary human osteoblast-like (HOB) cells obtained from trabecular bone by surgical operations (Promocell GmbH, Germany) were used to study the biocompatibility of SiHA coated Ti. These cells were cultured in McCoy's 5A medium containing 10% foetal calf serum, 1% glutamine and Vitamin C (30 μg/ml). SiHA coatings of different compositions were sterilised in ethanol for 48 h before treatment with ultra-violet radiation for 30 min. HOB cells (1×10^4 cells/test) were then seeded on the surface of SiHA coatings and uncoated Ti (acting as a control) before incubating at 37°C in a humidified atmosphere of 95% air and 5% carbon dioxide.

At days 2, 4 and 7, the metabolic activity of the cells on each specimen was determined by the alamarBlue™ assay (Serotec, Oxford, UK). The absorbance was measured on a plate reader at a wavelength of 570 nm with a reference wavelength of 600 nm. A total of 6 replications were performed for each specimen. A t-test was used to determine whether any significant differences existed between the mean values of the experimental groups. Differences between groups was considered to be significant at $p<0.05$.

After culturing for 1 day, HOBs were fixed with 4% paraformaldehyde/phosphate buffer solution (PBS) with 1% sucrose for 15 min, washed with PBS and permeabilised at 4°C for 5 min. Following that, cells were incubated with 1% bovine serum albumin (BSA)/PBS at 37°C for 5 min to block the non-specific binding. FITC conjugated phalloidin (1:100 in 1% BSA/PBS, Sigma, Poole, UK) was then added at 37°C for 1 h. After washing three times with 0.5% Tween 20/PBS for 5 min, TOTO-3 (1:5000 in Tris/EDTA buffer at pH 8.0, Molecular Probes, Paisley, UK) was added at 24°C for 5 min. The cells were then given a final wash (5 min×3) before mounting on the Vectorshield fluorescent mountant (Vector Laboratories, Peterborough, UK) and viewed under a Leica SP2 Confocal Laser Scanning Microscope. After 2 and 16 days in culture, the specimens were rinsed with PBS before freeze-drying. They were then coated with a thin layer of carbon. The morphology of HOB cells was examined using FE-SEM.

3. Results and discussion

3.1. Physicochemical properties of SiHA

HA thin coatings containing various levels of Si substitution were produced via magnetron co-sputtering at

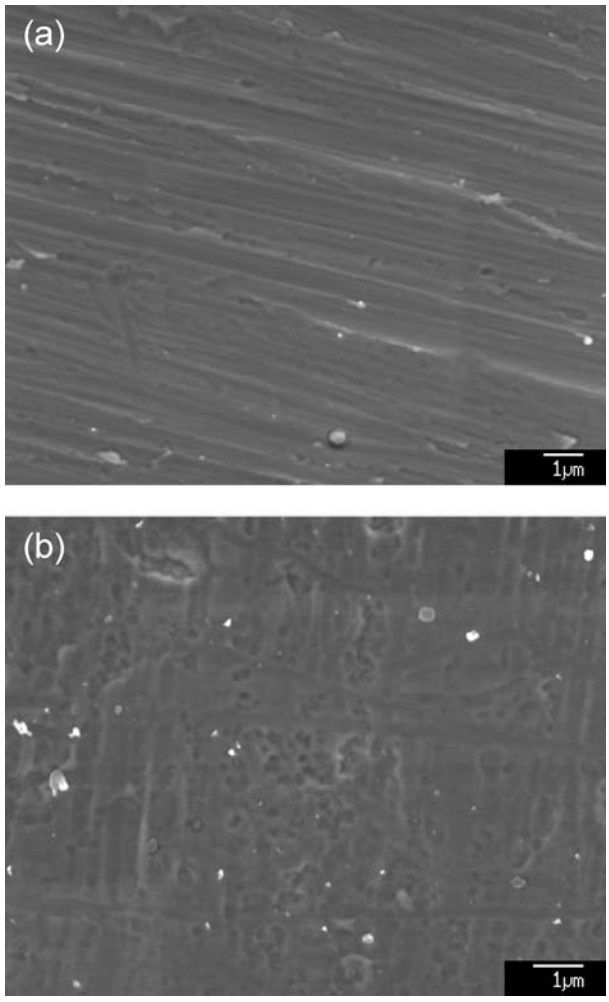

Figure 2 Morphology of a typical SiHA thin coating obtained by magnetron co-sputtering technique. (a) As-deposited 0.8 wt.% Si; (b) Heat-treated 0.8 wt.% Si: black patches are the submicrometer-sized voids.

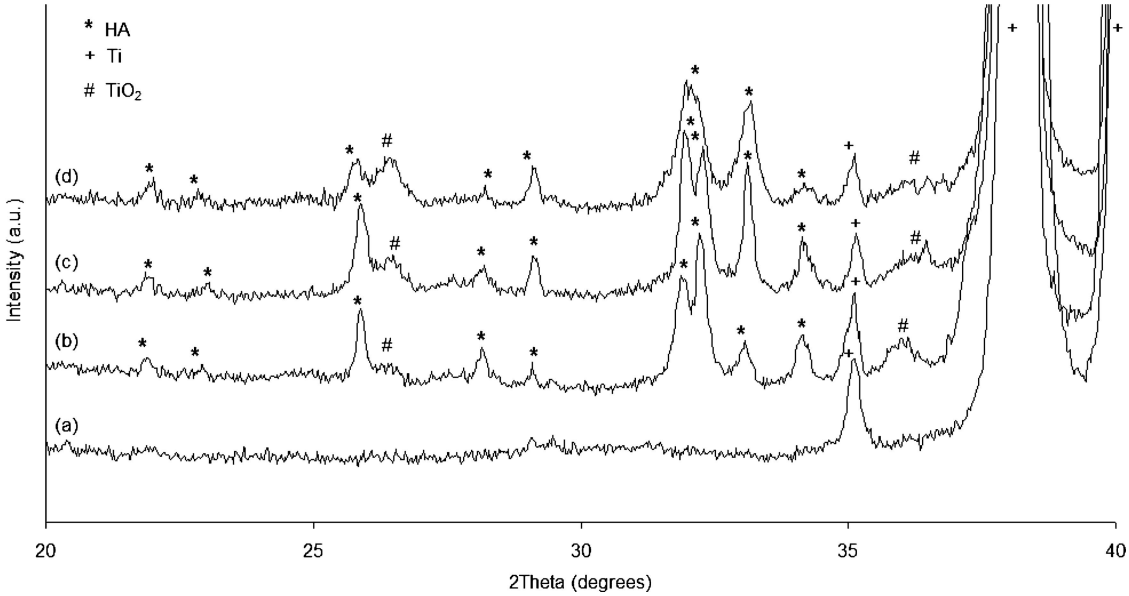

Figure 3 XRD patterns of SiHA thin coatings with varied Si content. (a) As-deposited 0.8 wt.% Si; (b) Heat-treated 0.8 wt.% Si; (c) Heat-treated 2.2 wt.% Si; (d) Heat-treated 4.9 wt.% Si.

room temperature, by carefully controlling the direct current (dc) power to the Si target. The Si content in the coating increased with increasing dc power whilst the radio frequency power to the HA target remained at 60 W. On the other hand, the coating thickness remained relatively constant (Table I). No significant changes in the Si content and coating thickness were detected after heat-treatment.

As-deposited coatings consisted of a homogenous, dense SiHA layer, with no cracks or other defects (Fig. 2a). Parallel lines from substrate grinding could be seen on the surface. In contrast, patches of submicrometre-sized voids could be observed on the heat-treated surface, rendering the coating to be partly porous (Fig. 2b). A decrease in both the Ca and P contents was observed. This may have been due to evaporation caused by the constant flow of moist argon gas during heat-treatment.

TABLE I Physicochemical properties of SiHA thin coatings

				Cell parameters[e]	
DC (W)[a]	Si (wt.%)[b]	t (μm)[c]	d (nm)[d]	a (nm)	c (nm)
3	0.8	0.7	50	0.9436 (7)	0.6915 (9)
9	2.2	0.7	34	0.9451 (7)	0.6938 (7)
15	4.9	0.7	19	0.9466 (9)	0.6956 (2)

[a]Direct current power source at Si target.
[b]Silicon composition determined by Energy Dispersive X-ray Spectrometer.
[c]Coating thickness measured by profilometer.
[d]Crystallite size determined by Scherrer equation using (001) plane of HA after heat-treatment.
[e]Cell parameters are determined after heat-treatment. Errors are ± standard errors of the mean, with the values in parentheses.

The amorphous nature of the as-deposited coatings with various Si contents was inferred from the XRD pattern (Fig. 3a). No crystalline peaks other than Ti (from the substrate) were observed. Following heat-treatment, nanocrystalline coatings were obtained, exhibiting sharp HA peaks (Figs. 3b–d). These lattice plane reflections became broader and less intense when the Si content increased. There was no evidence of secondary phases such as tricalcium phosphate (TCP), tetracalcium phosphate (TTCP) or calcium oxide (CaO) in any of the XRD patterns, within the detection limits. With increasing Si addition, the crystallite size of SiHA decreased (Table I). These results are in agreement with those of bulk SiHA, for which Si incorporation inhibited grain growth, the effect being more significant as the level of Si increased [43, 44]. As such, it could be expected that increased Si amount would cause HA crystals to be more soluble, releasing more Ca^{2+} and P^{5+} ions into the culture medium; thus rapidly re-precipitating and developing a newly-formed CaP-rich layer on the coating surface, with features very similar to the mineral phase found in bone; hence providing an ideal site for the osteoblast (bone-forming) cells to attach, grow and form new bone [45].

Substitution of Si ions into the apatite structure resulted in a change in the cell parameters of the heat-treated coatings (Table I). In the present study, both the a- and c-axes increased with Si substitution, following the trend in bulk SiHA as described by Kim *et al.* [46]. These changes

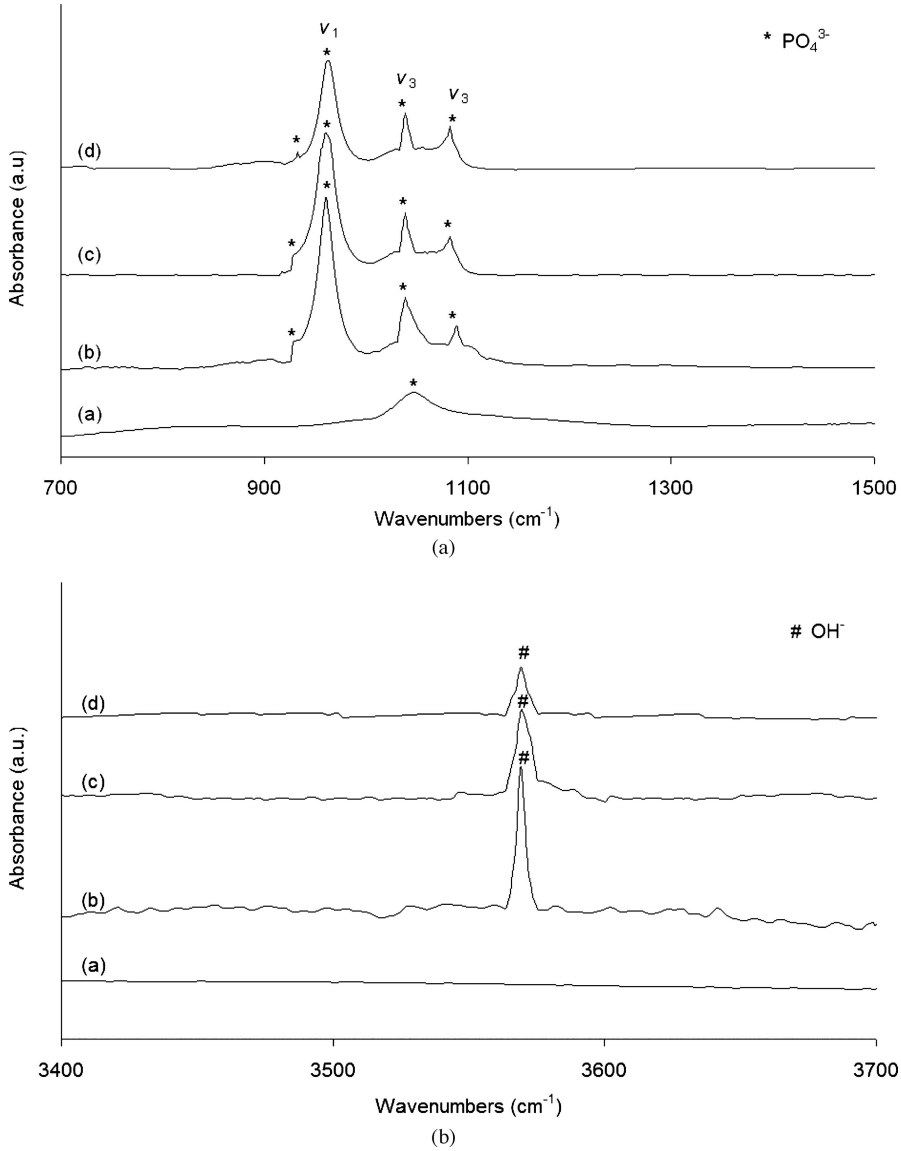

Figure 4 FTIR spectra of SiHA thin coatings with varied Si content. (a) As-deposited 0.8 wt.% Si; (b) Heat-treated 0.8 wt.% Si; (c) Heat-treated 2.2 wt.% Si; (d) Heat-treated 4.9 wt.% Si.

in the unit cell parameters became more apparent with increasing Si concentration. These findings are logical since the ionic radius of Si^{4+} (0.042 nm) is larger than P^{5+} (0.035 nm). However, although the addition of Si increased the cell parameters and reduced the crystallite size, the X-ray data showed no changes in the relative intensities. Such changes are normally expected when there is an atomic substitution, but not for this case, since Si and P are adjacent in the Periodic Table (and differ by only 1 in atomic number) and the Si level is relatively low (<5 wt.%).

All the as-deposited coatings exhibited very similar FTIR spectra (Fig. 4a): one broad adsorption band at 1038 cm^{-1}, associated with the presence of P–O. Heat-treatment led to several changes in the spectra (Fig. 4b–d). The band at 3571 cm^{-1}, which corresponds to the stretching mode of O–H, appeared as a sharp peak. The former v_3 P–O stretching mode centred at 1038 cm^{-1} became intense and sharper. Three new bands also appeared: one at 1089 cm^{-1}, which was assigned to v_3 P–O stretching mode, the second at 962 cm^{-1}, which was assigned to v_1 stretching mode, and the other at 935 cm^{-1}, which could be related to the presence of Si in the apatite [47, 48]. These changes signified the formation of a well-crystallised HA phase after heat-treatment. Although all of the FTIR spectra showed absorption bands characteristic of HA, the band intensities corresponding to O–H and P–O (most noticeably at 962 cm^{-1}) decreased as the Si content increased.

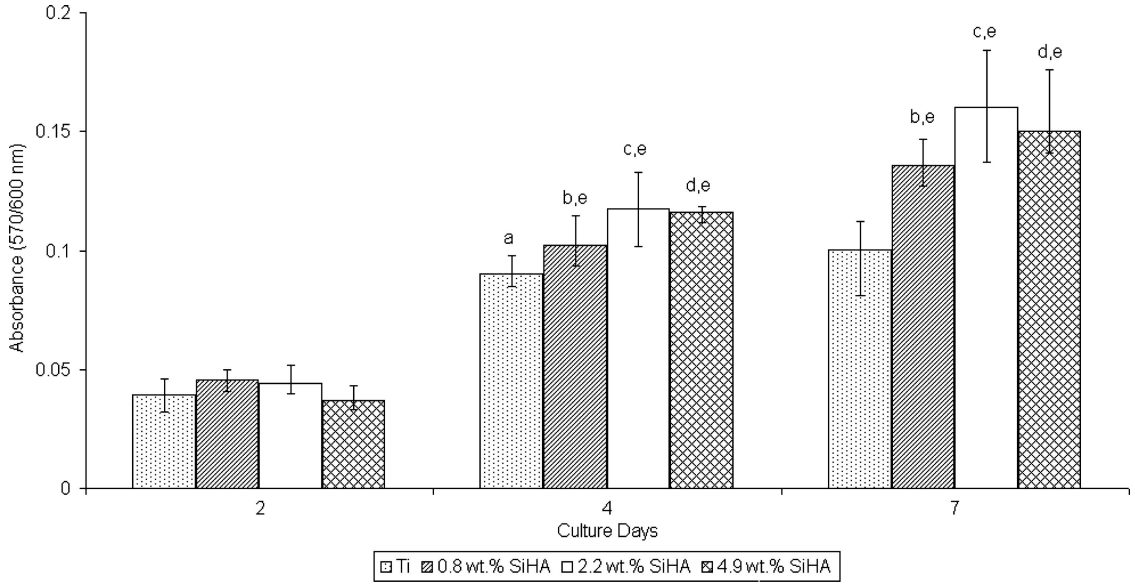

Figure 5 Growth of HOB cells on various specimens. [a]$p < 0.05$: Growth activity of cells was significantly higher on uncoated Ti between day 2 and 4; [b]$p < 0.05$: Growth activity of cells was significantly higher on 0.8 wt.% SiHA between day 2 and 4, and day 4 and 7; [c]$p < 0.05$: Growth activity of cells was significantly higher on 2.2 wt.% SiHA between day 2 and 4, and day 4 and 7; [d]$p < 0.05$: Growth activity of cells was significantly higher on 4.9 wt.% SiHA between day 2 and 4, and day 4 and 7; [e]$p < 0.05$: Growth activity was significantly higher for cells grown on SiHA than uncoated Ti within days 4 and 7.

These results suggest that from the physical and chemical viewpoints, the addition of Si into HA resulted in a stoichiometric coating. It appears that Si^{4+} ions are structurally incorporated into the HA lattice in solid solution, and are not segregated as a second phase. The phosphate tetrahedra were replaced by the silicate tetrahedra in the HA structure, owing to a decrease in P–O intensity with increasing substituted Si. Thus, the mechanism in which substitution of Si into the HA lattice $[Ca_{10}(PO_4)_{6-x}(SiO_4)_x(OH)_{2-x}]$ as proposed by Gibson *et al*. [47] is confirmed by the reduction in the O–H FTIR peak intensity at 3571 cm^{-1} with increasing Si concentration, as observed in Fig. 3.

The amount of substituted Si in SiHA coatings that can be achieved using magnetron co-sputtering and as observed in this study is of particular interest. This is the first report of substituted Si levels as high as 4.9 wt.%, incorporated within the HA structure whilst retaining phase purity. This achievement is attributed to the stringent control and selection of the processing parameters and conditions, to prevent the formation of carbonated HA since SiO_4^{4-} and CO_3^{2-} ions are known to replace PO_4^{3-} competitively [47, 49].

3.2. Biological properties of SiHA

The growth activity of HOB cells on both uncoated Ti and Ti surfaces coated with SiHA increased significantly from days 2 to 7, and from days 2 to 4, respectively (Fig. 5). HOB cells tend to multiply significantly on all SiHA coatings as compared to uncoated Ti at days 4 and 7, indicating the excellent bioactivity of SiHA material.

Immunofluorescence staining revealed that HOBs displayed well-oriented, flattened cytoskeletons with clear evidence of actin stress fibres along the substrate grinding, by day 1 on all coatings (Fig. 6a). Furthermore, cell nuclei were considered to exhibit normal phenotype morphology, revealing several chromosomes and were capable of cell division. Cells maintained their typical osteoblastic morphology throughout the culture period on all coated surfaces. By day 2, HOBs were seen attaching and spreading across the coating surfaces, and growing as well-flattened monolayers (Fig. 6b). In addition, synthesis of extracellular matrix comprising of Ca and P (confirmed by spot EDS analysis), were formed throughout beneath the cell layers (Fig. 6c). Multilayers of cells, with extensions as long as 10 μm in length, were observed by day 16 (Fig. 6d). All these results provide evidence that SiHA thin coatings produced favourable biological response *in vitro*.

Surface modification of Ti with SiHA coatings is an alternative way to produce bioactive implants. The enhanced bioactivity was attributed to the combined effects: the presence of HA which promoted cell attachment and growth; and the incorporation of Si into HA which appeared to stimulate the cell activity. The presence of released Si in the culture medium due to dissolution of SiHA was hypothesised to affect the regulators of DNA synthesis in the HOBs, and in turn, have stimulatory effect on the bone mineralisation process. This effect was likely to be a possible explanation, although the actual mechanism by which Si affects the cell activity requires further investigation.

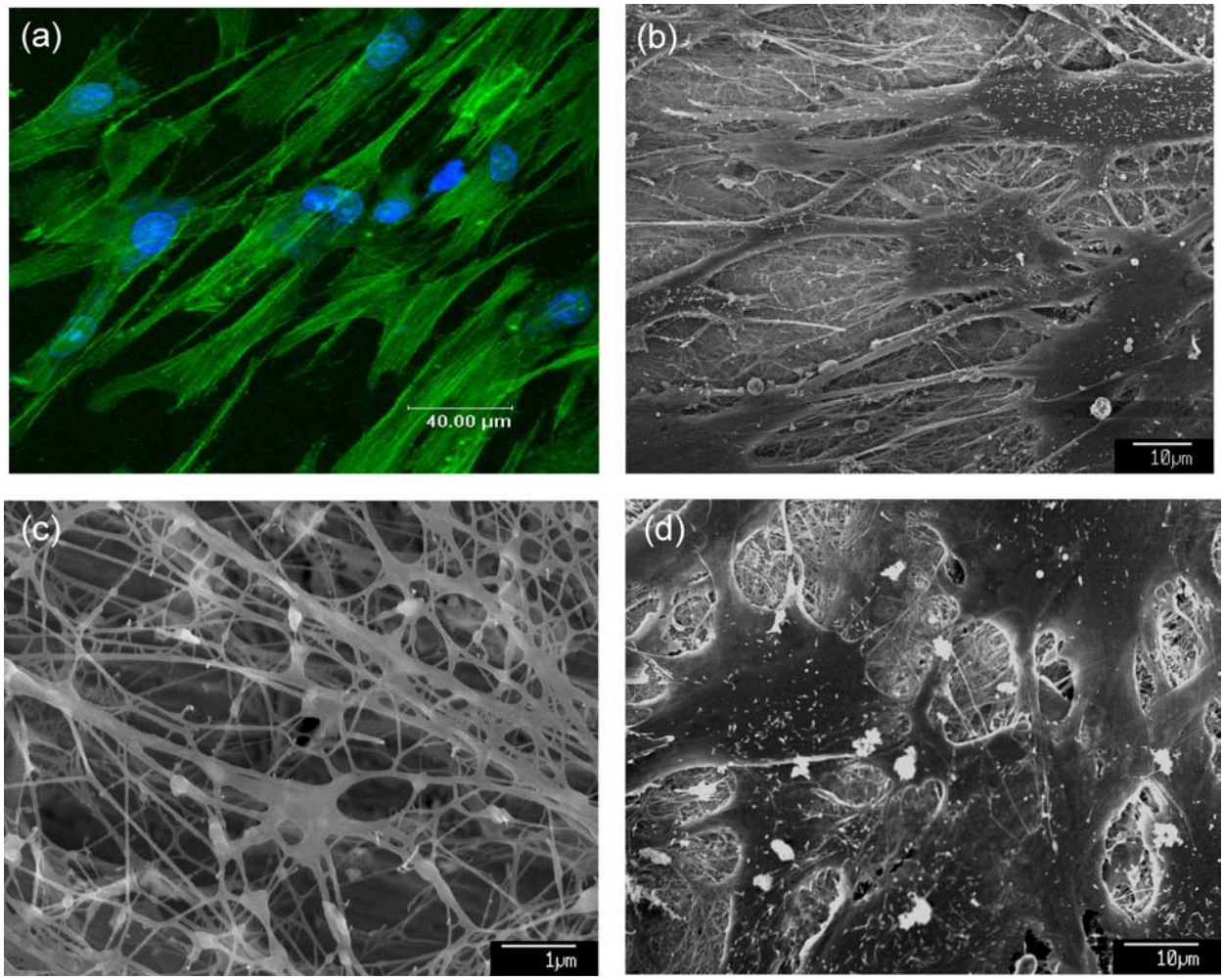

Figure 6 Images of human osteoblast-like (HOB) cells on heat-treated SiHA thin coating. (a) Actin cytoskeletons (stained green) and cell nuclei (stained blue) of HOBs by day 1: 0.8 wt.% Si; (b) Monolayer of cells attaching and spreading across the surface by day 2: 0.8 wt.% Si; (c) Evidence of extracellular matrix synthesis by day 2: 4.9 wt.% Si; (d) Formation of multilayer of cells by day 16: 0.8 wt.% Si.

4. Conclusions

A novel method for synthesising thin coatings of SiHA has been demonstrated. Thin coatings (∼1 μm thick) of SiHA were produced by the magnetron co-sputtering technique. The as-deposited coatings were amorphous, with varying Si content up to 4.9 wt.%. Nanocrystalline, single-phase SiHA thin coatings that retained their HA crystallographic structure, were achieved following heat-treatment at 600°C for 3 h. In addition, the unit cell parameters (both *a*- and *c*-axes) increased and the crystallite size decreased, with increasing Si addition. The *in vitro* cellular response indicated an increase in the growth of HOB cells on these coatings, along with the formation of extracellular matrix. Furthermore, immunofluorescent staining revealed that the cytoskeletons on SiHA showed clear evidence of well-formed actin stress fibres. All these observations confirmed the enhanced bioactivity and biofunctionality of SiHA thin coatings.

Acknowledgements

The authors wish to acknowledge the use of the EPSRC's Chemical Database Service at Daresbury [50]. This work was supported by Girton College, Cambridge; Cambridge Commonwealth Trust; Lee Foundation, Singapore; and Sir Richard Stapley Educational Trust on behalf of GlaxoSmithKline plc., United Kingdom.

References

1. L. L. HENCH, *Science* **208** (1980) 826.
2. K. DE GROOT, J. G. C. WOLKE and J. A. JANSEN, *Proc. Instn. Mech. Engrs.* **212H** (1998) 137.
3. A. S. POSNER, A. PERLOFF and A. F. DIORIO, *Acta. Crystall.* **11** (1958) 308.
4. S. SINGH, S. P. TRIKHA and A. J. EDGE, *J. Bone Joint Surg.* **86B** (2004) 1118.
5. R. J. FURLONG and J. F. OSBORN, *ibid.* **73B** (1991) 741.

6. R. G. T. GEESINK and N. H. M. HOEFNAGELS, *ibid.* **77B** (1995) 534.
7. W. R. LACEFIELD and L. L. HENCH, *Biomater.* **7** (1986) 104.
8. W. C. A. VROUWENVELDER, C. G. GROOT and K. DE GROOT, *ibid.* **13** (1992) 382.
9. A. OLIVA, A. SALERNO, B. LOCARDI, V. RICCIO, F. DELLS RAGIONE, P. IARDINO and V. ZAPPIA, *ibid.* **19** (1998) 1019.
10. C. GABBI, A. CACCHIOLI, B. LOCARDI and E. GUADAGNINO, *ibid.* **16** (1995) 515.
11. M. NAGASE, Y. ABE, M. CHIGIRA and E. UDAGAWA, *ibid.* **13** (1992) 172.
12. J. E. GOUGH, D. C. CLUPPER and L. L. HENCH, *J. Biomed. Mater. Res.* **69A** (2004) 621.
13. J. E. GOUGH, J. R. JONES and L. L. HENCH, *Biomater.* **25** (2004) 2039.
14. J. W. M. VEHOF, J. D. D. S. MAHMOOD, H. TAKITA, M. A. VAN'T HOF, Y. KUBOKI, P. H. M. SPAUWEN and J. A. JANSEN, *Plast. and Reconstr. Surg.* **108** (2001) 434.
15. M. LIND, S. OVERGAARD, T. NGUYEN, B. ONGPIPATTANAKUL, C. BUNGER and K. SOBALLE, *Acta. Orthop. Scand.* **67** (1996) 611.
16. M. YAZDI, S. BERNICK and W. J. PAULE, *Clin. Orthop.* **262** (1991) 281.
17. T. J. WEBSTER, C. ERGUN, R. H. DOREMUS and R. BIZIOS, *J. Biomed. Mater. Res.* **59** (2002) 312.
18. A. E. PORTER, N. PATEL, J. N. SKEPPER, S. M. BEST and W. BONFIELD, *Biomater.* **24** (2003) 4609.
19. N. PATEL, I. R. GIBSON, K. A. HING, S. M. BEST, E. DAMIEN, P. A. REVELL and W. BONFIELD, *Key Eng. Mater.* **218–220** (2002) 383.
20. J. R. FARLEY, J. E. WERGEDAL and D. J. BAYLINK, *Science* **222** (1983) 330.
21. E. M. CARLISLE, *ibid.* **167** (1970) 279.
22. *Idem.*, *ibid.* **178** (1972) 619.
23. *Idem.*, *Fed. Proc.* **32** (1973) 930.
24. *Idem.*, *J. Nutr.* **110** (1980) 1046.
25. D. M. REFFITT, N. OGSTON, R. JUGDAOSHSINGH, H. F. J. CHEUNG, B. A. J. EVANS, R. P. H. THOMPSON, J. J. POWELL and G. N. HAMPSON, *Bone* **32** (2003) 127.
26. I. R. GIBSON, K. A. HING, P. A. REVELL, J. D. SANTOS, S. M. BEST and W. BONFIELD, *Key Eng. Mater.* **218–220** (2002) 203.
27. A. E. PORTER, N. PATEL, J. N. SKEPPER, S. M. BEST and W. BONFIELD, *Biomater.* **25** (2004) 3303.
28. N. PATEL, S. M. BEST, W. BONFIELD, I. R. GIBSON, K. A. HING, E. DAMIEN and P. A. REVELL, *J. Mater. Sci. Mater. Med.* **13** (2002) 1199.
29. E. S. THIAN, J. HUANG, S. M. BEST, Z. H. BARBER and W. BONFIELD, *Biomater.* **26** (2005) 2947.
30. *Idem.*, *J. Mater. Sci. Mater. Med.* **16** (2005) 411.
31. L. SUN, C. C. BERNDT, K. A. GROSS and A. KUKCUK, *J. Biomed. Mater. Res. (Appl. Biomater.)* **58** (2001) 570.
32. K. DE GROOT, R. G. T. GEESINK, C. P. A. T. KLEIN and P. SEREKIAN, *J. Biomed. Mater. Res.* **21** (1987) 1375.
33. A. MORONI, V. L. CAJA, C. SABATO, E. L. EGGER, F. GOTTSAUNER-WOLF and E. Y. S. CHAO, *J. Mater. Sci.: Mater. Med.* **5** (1994) 411.
34. A. MORONI, S. TOKSVIG-LARSEN, M. C. MALTARELLO, L. ORIENTI, S. STEA and S. GIANNINI, *J. Bone Joint Surg.* **80A** (1998) 547.
35. S. R. RADIN and P. DUCHEYNE, *J. Mater. Sci. Mater. Med.* **3** (1992) 33.
36. M. J. FILLIAGGI, N. A. COOMBS and R. M. PILLIAR, *J. Biomed. Mater. Res.* **25** (1991) 1211.
37. P. DUCHEYNE, S. RADIN and L. KING, *ibid.* **27** (1993) 25.
38. K. A. GROSS, C. C. BERNDT, D. D. GOLDSCHLAG and V. J. IACONO, *Int. J. Oral & Maxillofac. Implants* **12** (1997) 589.
39. E. W. MORSCHER, A. HEFTI and U. AEBI, *J. Bone Joint Surg.* **80B** (1998) 267.
40. M. ROKKUM, A. REIGSTAD and C. B. JOHANSSON, *Acta Orthop. Scand.* **73** (2002) 298.
41. D. B. WILES and R. A. YOUNG, *J. Appl. Cryst.* **14** (1981) 149.
42. I. KAY, R. A. YOUNG and A. S. POSNER, *Nature* **204** (1964) 1050.
43. I. R. GIBSON, S. M. BEST and W. BONFIELD, *J. Am. Ceram. Soc.* **85** (2002) 2771.
44. D. ARCOS, J. RODRIGUEZ-CARVAJAL and M. VALLET-REGI, *Chem. Mater.* **16** (2004) 2300.
45. M. NEO, T. NAKAMURA, C. OHTSUKI, T. KOKUBO and T. YAMAMURO, *J. Biomed. Mater. Res.* **27** (1993) 999.
46. S. R. KIM, J. H. LEE, Y. T. KIM, D. H. RIU, S. J. JUNG, Y. J. LEE, S. C. CHUNG and Y. H. KIM, *Biomater.* **24** (2003) 1389.
47. I. R. GIBSON, S. M. BEST and W. BONFIELD, *J. Biomed. Mater. Res.* **44** (1999) 422.
48. T. h. LEVENTOURI, C. E. BUNACIU and V. PERDIKATSIS, *Biomater.* **24** (2003) 4205.
49. I. R. GIBSON and W. BONFIELD, *J. Biomed. Mater. Res.* **59** (2002) 697.
50. D. A. FLETCHER, R. F. MCMEEKING and D. PARKIN, *J. Chem. Inf. Comput. Sci.* **36** (1996) 746.